**BNL-90574-2009-CP**

# *Future BNL plans for a polarized electron-ion collider (eRHIC)*

**Christoph Montag**

*Presented at the Advanced Studies Institute – Symmetries and Spin (SPIN-Praha-2009)*
Charles University, Prague, Czech Republic
July 26 – August 2, 2009

**Collider-Accelerator Department**

**Brookhaven National Laboratory**
P.O. Box 5000
Upton, NY 11973-5000
www.bnl.gov

# DISCLAIMER

# Future BNL plans for a polarized electron-ion collider (eRHIC)

Christoph Montag

Brookhaven National Laboratory, Upton, NY 11973, USA

**Abstract.** To provide polarized electron-proton collisions of $\sqrt{s} = 100\,\mathrm{GeV}$, addition of a 10 GeV electron accelerator to the existing RHIC facility is currently under study. Two design lines are under consideration: a self-polarizing electron ring, and an energy recovery linac. While the latter provides significantly higher luminosities, it is technologically very challenging. We present both design approaches and discuss their advantages and limitations.

## 1 Introduction

The polarized electron-ion collider eRHIC at Brookhaven will provide collisions between 10 GeV polarized electrons and 250 GeV polarized protons or 100 GeV/nucleon heavy ions. Later upgrades may provide higher lepton and hadron beam energies. Two main design choices achieve this: a ring-ring scheme and a linac-ring design. Each of these two choices has its distinct advantages and disadvantages. For instance, with a few modifications, an electron-ring based design can provide positrons as well, which may be desirable for certain experiments. On the other hand, reducing the hadron beam energy requires a significant electron ring circumference modification due to the hadron beam velocity change. In an electron-linac based design, the required adjustment can be done more easily with a slight linac RF frequency change. However, a linac-based design will not be capable of providing positron beams, since positrons cannot be generated at sufficient intensities.

In the following sections, we discuss the present status of these two approaches at Brookhaven.

## 2 Ring-ring

The eRHIC ring-ring design [1] consists of a 10 GeV self-polarizing electron storage ring colliding with one of the existing RHIC beams in a single interaction point (IP). A full-energy injector is foreseen to facilitate trickle-injection, therefore keeping the electron beam intensity constant during a store. Table 1 lists the design parameters of the ring-ring based scheme.

The luminosity of the ring-ring version is limited by the beam-beam effect on the electron beam. The strength of this highly nonlinear kick, which has the form

$$F_x + iF_y = \sqrt{\frac{2\pi}{\sigma_x^2 - \sigma_y^2}} \left[ w\left( \frac{x+iy}{\sqrt{2(\sigma_x^2-\sigma_y^2)}} \right) - \exp\left( -\frac{x^2}{2\sigma_x^2} - \frac{y^2}{2\sigma_y^2} \right) w\left( \frac{\frac{\sigma_y}{\sigma_x}x + i\frac{\sigma_x}{\sigma_y}y}{\sqrt{2(\sigma_x^2-\sigma_y^2)}} \right) \right], \tag{1}$$

$$w(z) \equiv \exp(-z^2)[1 - \mathrm{erf}(-iz)], \tag{2}$$

| | unit | no cooling | pre-cooling |
|---|---|---|---|
| $\epsilon_p$ | nm | 9.5 | 3.8 |
| $\epsilon_e$ $(x/y)$ | nm | 53/9.5 | 21/3.8 |
| $N_b$ | | 166 | 166 |
| $f_{\mathrm{rev}}$ | kHz | 78 | 78 |
| $E_p$ | GeV | 250 | 250 |
| $E_e$ | GeV | 10 | 10 |
| $N_e$ | | $2.3 \cdot 10^{11}$ | $0.9 \cdot 10^{11}$ |
| $N_p$ | | $2 \cdot 10^{11}$ | $1.6 \cdot 10^{11}$ |
| $\beta_p^*$ (x/y) | m | 1.08/0.27 | 0.43/0.11 |
| $\beta_e^*$ (x/y/) | m | 0.19/0.27 | 0.08/0.11 |
| $\xi_p$ $(x/y)$ | | 0.015/0.008 | 0.015/0.008 |
| $\xi_e$ $(x/y)$ | | 0.06/0.16 | 0.12/0.32 |
| L | $\mathrm{cm}^{-2}\mathrm{sec}^{-1}$ | $9.5 \cdot 10^{32}$ | $1.8 \cdot 10^{33}$ |

**Table 1.** Design parameters of the eRHIC ring-ring design.

is characterized by the beam-beam parameter

$$\xi_{x,y} = \frac{N r_e \beta^*_{x,y}}{2\pi\gamma\sigma_{x,y}(\sigma_x + \sigma_y)}. \tag{3}$$

Typical limitations are around $\xi = 0.15$ for electron beams, and $\xi = 0.02$ for hadrons.

However, recent simulation studies indicate that this nonlinear beam-beam kick can be at least partially compensated [2]. If, immediately after the interaction with the hadron beam, a kick of the same strength but opposite sign could be applied to the electron beam, the net kick would be exactly zero. In reality, the compensation device cannot be placed immediately after the electron-hadron interaction point. Instead, it will be located at some distance from the IP, with an appropriate transport channel in-between. This transport channel will be nonlinear due to the presence of chromaticity sextupoles.

These simulation studies were carried out on a simplified model storage ring, consisting of 50 FODO cells. The electron lens is separated from the IP by an arc comprised of 10 FODO cells. All FODO cells are equipped with sextupoles to correct the (linear) chromaticity. Low-$\beta$ focusing at the IP and the electron lens is provided by chromatic telescopes.

Tune scans with and without head-on beam-beam compensation show a dramatic improvement in the attainable peak luminosity and in the available tune space (Fig. 1) [2]. While the beam-beam interaction leads to a huge emittance blow-up of the electron beam without the electron lens, manifesting itself in a significant reduction of the luminosity to about 30-40 percent of the nominal value even at the optimum working point, the corresponding luminosity with beam-beam compensation is around 60-70 percent of the nominal value over a wide tune range.

The formation of long, non-Gaussian transverse tails is referred to as the second beam-beam limit. Simulations show that the electron lens significantly reduces these non-Gaussian tails, as depicted in Fig. 2 [2].

In a real collider, intensities and emittances vary on a bunch-by-bunch basis. It is therefore necessary to ensure a sufficient robustness of the head-on beam-beam compensation scheme against such variations, as well as against machine imperfections such as spurious dispersion or beam-beam offsets at the IP and/or the electron lens. Simulation studies indicate that the most sensitive parameter is the betatron phase advance between the IP and the electron lens, which has to be controlled within 2°.

To preserve the self-polarizing properties of the electron storage ring at energies below the nominal design energy of 10 GeV, the bending dipoles are designed as superbends [3]. In this scheme, each dipole is comprised of three magnets. At the highest energy, all dipoles are excited at the same field levels to limit the amount of synchrotron radiation to manageable levels. At lower energies, only the center dipole is powered. The smaller bending radius results

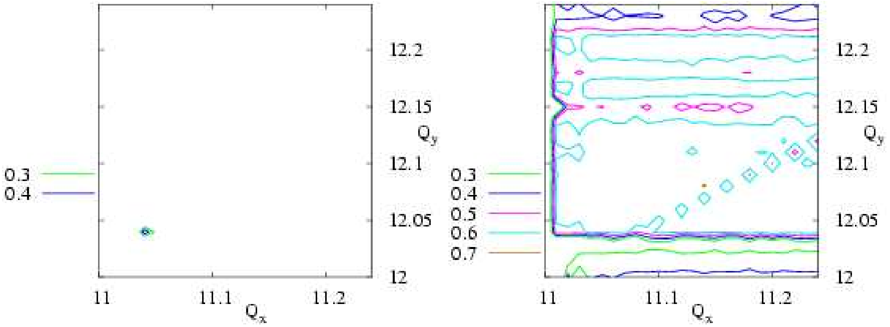

**Fig. 1.** Contour plots of tune scans for the eRHIC ring-ring version, with (right) and without (left) head-on beam-beam compensation.

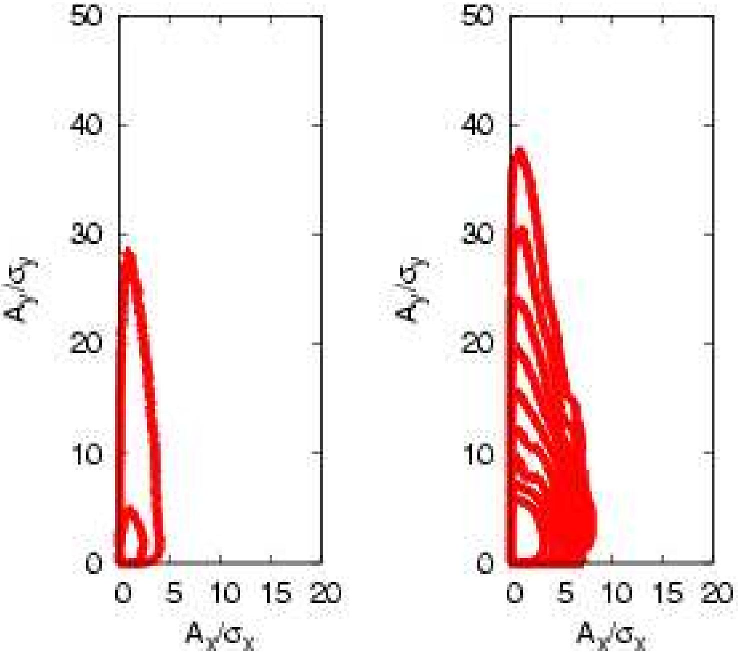

**Fig. 2.** Transverse electron distributions for the eRHIC ring-ring version, with (right) and without (left) head-on beam-beam compensation. Each contour line corresponds to a factor 10.

in the generation of an enhanced amount of synchrotron radiation, shortening the polarization build-up time.

## 3 Linac-ring

In the linac-ring scheme [1] a linac provides the electron beam for collisions with the hadrons stored in RHIC. With a design beam energy of 10 GeV and a beam current of several hundred milliamps, the beam power of several gigawatts needs to be recovered for this scheme to be economically feasible. This is accomplished in an energy-recovery linac (ERL) [4], where the spent electron beam after the collision point re-enters the superconducting linac with a phase shift of 180° relative to the RF phase. This leads to a deceleration of the beam in the linac, and the beam power is recovered to a high degree. To limit the length and cost of the superconducting

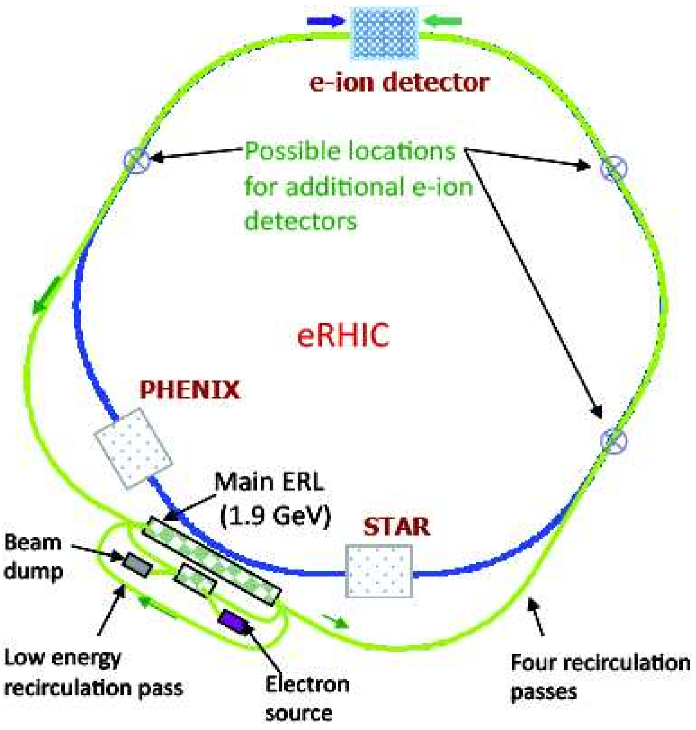

**Fig. 3.** eRHIC linac-ring scheme [5].

| | | high energy | | low energy | |
|---|---|---|---|---|---|
| | unit | p | e | p | e |
| energy | GeV | 250 | 10 | 50 | 3 |
| bunch freq. | MHz | 14.1 | | 14.1 | |
| bunch int. | $10^{11}$ | 2.0 | 1.2 | 2.0 | 1.2 |
| beam current | A | 0.42 | 0.26 | 0.42 | 0.26 |
| emittance | nm | 3.8 | 5.0 | 19.0 | 16.5 |
| $\beta^*$ | cm | 26 | 20 | 26 | 30 |
| beam-beam parameter | | 0.015 | 0.6 | 0.015 | 0.47 |
| bunch length | cm | 20 | 1.0 | 20 | 1.0 |
| peak luminosity | $[10^{33}\,\mathrm{cm}^{-2}\mathrm{sec}^{-1}]$ | 2.6 | | 0.53 | |

**Table 2.** Parameters of the eRHIC linac-ring design.

linac, a 1.9 GeV linac with four recirculation loops is used, as shown in Fig. 3. The design parameters of this approach are listed in Table 2.

The main technological challenge of the linac-ring scheme is the high intensity polarized electron gun. Polarized electrons are generated by photo emission from a strained GaAs cathode, and accelerated by an RF cavity. Collisions of the accelerated electrons with residual gas molecules in the electron gun vacuum result in the generation of ions, which are subsequently accelerated by the RF field towards the cathode. This continuous bombardment of the cathode significantly reduces its quantum efficiency, and therefore its lifetime [8][9].

To ensure sufficient cathode lifetime at high intensities (about two orders of magnitude higher than what has been achieved), two different approaches are being pursued. The first approach uses multiple cathodes, with the electrons extracted from these being combined into a single beam by an RF combiner, Fig. 4 [10].

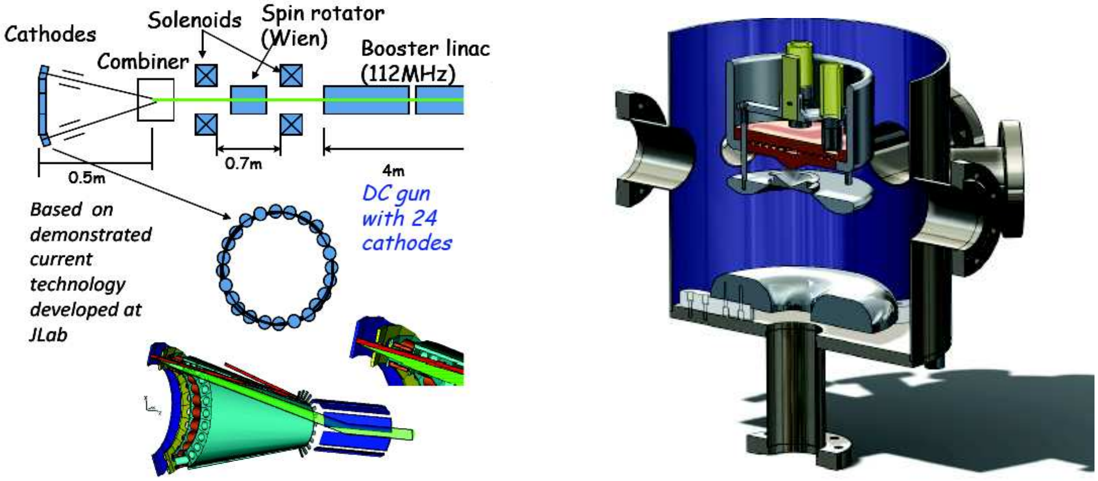

**Fig. 4.** High-intensity polarized electron gun schemes under consideration. Beams from multiple cathodes are combined to form a single linac beam (left) [10]. A single ring-shaped cathode is used to avoid cathode damage by ion back-bombardment [11], which occurs mainly in the center of the cathode (right).

**Fig. 5.** Photo of a superconducting 5-cell linac cavity.

The second approach takes advantage of the fact that the cathode damage occurs mainly in the center. With a ring-shaped cathode, the lifetime is expected to be orders of magnitude longer than with a conventional cathode [11].

Due to the high beam intensity and multiple recirculation loops, the total beam current in the linac is of the order of several amps. It is therefore mandatory to ensure that no instabilities arise from higher order modes excited by the beam in the superconducting cavities. A dedicated cavity design has been developed with large diameter irises and beam pipes that guide all higher order modes out of the cavity and into ferrite absorbers. Simulations show a beam break-up instability threshold of about 20 A for this cavity [12], which is roughly an order of magnitude higher than the actual total beam current. Figure 5 shows a photo of a prototype cavity.

Since beams of different energies are accelerated and decelerated in the same linac, beams of different energies need to be focused. Figure 6 shows the beamsize in the linac; the recirculating loops are modeled as simple matrices here [12]. Since space for the installation of the four return loops in the existing RHIC tunnel is very limited, compact C-shaped magnets have been

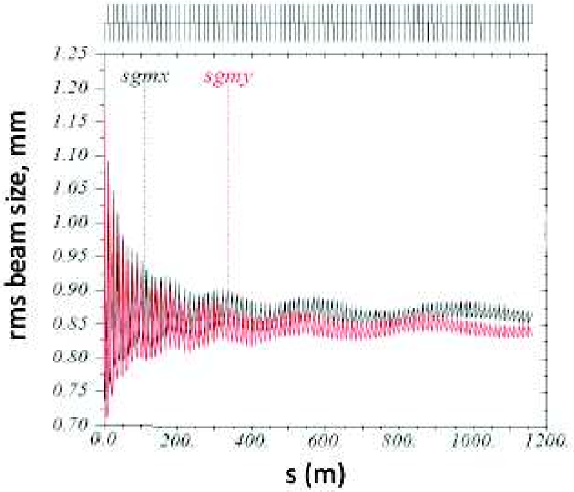

**Fig. 6.** Electron rms beam size during multiple passes through the linac. The recirculating arcs are modelled as thin-lens matrices.

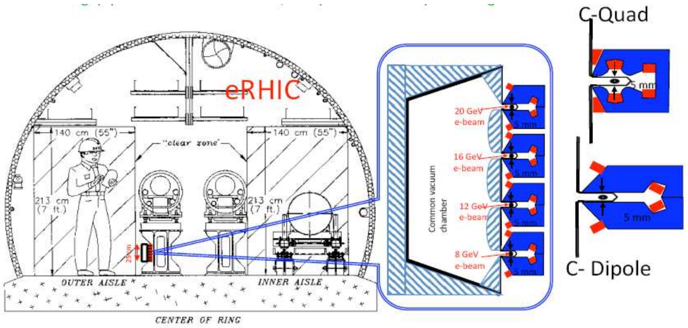

**Fig. 7.** Schematic view of the compact magnets with their common vacuum chamber for the four recirculating loops [13].

designed [13]. The magnets of the four return loops will be stacked on top of each other, and the beams will share a common vacuum chamber, as shown in Fig. 7. Synchrotron radiation from the bending magnets will be emitted into the common chamber, which is equipped with a dedicated synchrotron radiation absorber.

Though the electrons will be discarded after colliding with the hadron beam and subsequent deceleration, the beam-beam interaction cannot be completely ignored. At large disruption parameters the disturbance of the electron beam phase space distribution results in fast emittance blow-up of the hadron beam [14]. To avoid this, the electron beam $\beta$-function at the IP has to be squeezed down to 20 cm, resulting in a modest beam-beam tuneshift parameter $\xi = 0.5$. Matched beam sizes at the interaction point require an electron beam emittance of $\epsilon_e = 5\,\mathrm{nm}$. As a consequence, low-$\beta$ focusing magnets for the electron beam will be required in the vicinity of the IP, which has important consequences for the interaction region design.

The interaction of the linac electron beam with the stored proton beam may also give rise to the kink instability, a head-tail type instability of the long proton bunches driven by the electron beam. Landau damping provided by 8 units of chromaticity should be sufficient to suppress this instability, Fig. 8 [14].

A distinct feature of the linac-ring approach is its stageability. Initially, a low-energy version can be built at a fraction of the cost of the high-energy machine. Later, almost all the components, especially the superconducting linacs, can be re-used when the final high-energy

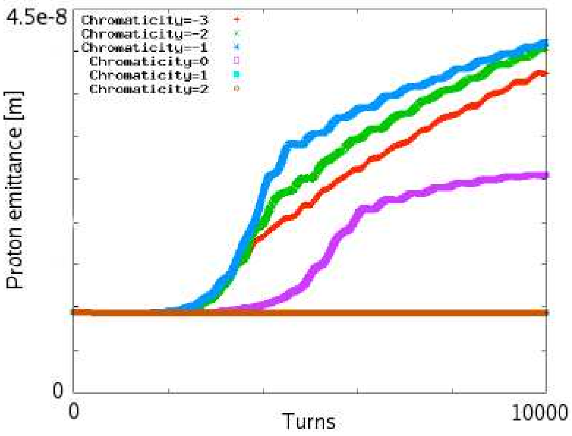

**Fig. 8.** Proton beam emittance evolution due to the kink instability, for different values of chromaticity [14].

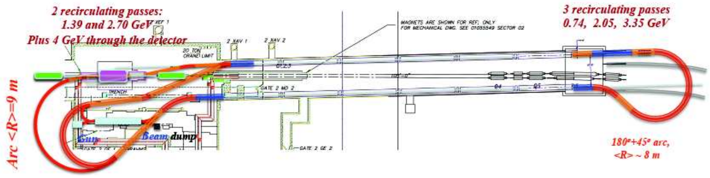

**Fig. 9.** Overview of the 4 GeV staged electron ERL MeRHIC [15].

collider is constructed. Most of the low-energy machine can be installed in an existing RHIC interaction region, as shown in Fig. 9, keeping the civil construction at a minimum [15].

## 4 Interaction region design

The design of the interaction region of eRHIC is very challenging. Electron and proton beams of vastly different energies have to be brought in collision at the interaction point, where beams have to be focused to small values of $\beta^*$ to maximize the luminosity. These small values of $\beta^*$ require the low-$\beta$ magnets to be placed as close as possible to the interaction point. This, in turn, requires the two beams to be separated close to the interaction point to be passed through their respective focusing magnets. This separation is accomplished by application of magnetic dipole fields. Due to the energy difference of the two beams, the electron beam is deflected away from the proton beam. This deflection results in the generation of several kilowatts of synchrotron radiation close to the interaction point. This synchrotron radiation fan has to be accomodated in the interaction region to avoid unacceptably high detector background levels. Figure 10 shows the geometry of the eRHIC interaction region.

## 5 Summary

Both the ring-ring and the linac-ring design approach for a future RHIC-based electron-ion collider provide exciting physics experiments. While the ring-ring approach is rather conservative, the ambitious linac-ring design is capable of providing significantly higher luminosity, using a number of new technological concepts. The final decision for one of the designs will be based on both the projected cost and the physics potential.

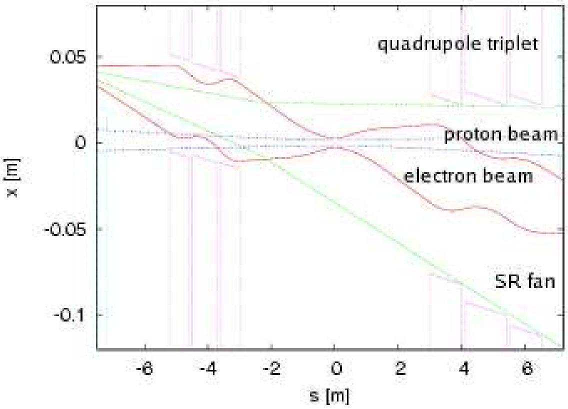

**Fig. 10.** Geometry of the eRHIC interaction region with the proton (blue) and electron beam (red), the synchrotron radiation fan (green), and the low-$\beta$ quadrupole triplets (magenta).

## References

1. M. Farkhondeh and V. Ptitsyn (eds.), C-A/AP/142, 2004
2. C. Montag and W. Fischer, Phys. Rev. ST Accel. Beams 12, 084001, 2009
3. A.V. Otboev, Yu.M. Shatunov, V. Ptitsyn, Nucl. Instrum. Meth. A536, 319-322, 2005
4. M. Tigner, Nuovo Cim. 37 (1965) 1228
5. http://www.bnl.gov/cad/eRhic/erhic.asp
6. E. Tsentalovich, AIP Conf. Proc. 980, 79-84, 2008
7. R. Calaga et al., Nucl. Instrum. Meth. A 557, 243-249, 2006
8. E. Pozdeyev et al., Phys. Rev. ST Accel. Beams 12, 043501, 2009
9. E. Pozdeyev, Proc. PAC07, 1356
10. V. Litvinenko, private communication
11. E. Tsentalovich, private communication
12. E. Pozdeyev, private communication
13. W. Meng et al., Proc PAC09, MO6PFP004
14. Y. Hao et al., Proc. PAC07, 1865
15. V. Ptitsyn et al., Proc. PAC09, WE6PFP062
16. C. Montag et al., Proc. PAC05, 2893